Canadian Journal of Remote Sensing, 41:431–439, 2015

ISSN: 0703-8992 print / 1712-7971 online
DOI: 10.1080/07038992.2015.1104636

Technical Note

Evaluation of RADARSAT-2 Acquisition Modes for Wetland Monitoring Applications

Brian Brisco[1], Kevin Murnaghan[1], Shimon Wdowinski[2], and Sang-Hoon Hong[2,3]*

[1]*Canada Centre for Remote Sensing Division, Natural Resources Canada, 560 Rochester Street, Ottawa, Ontario K1A 0E4, Canada*

[2]*Division of Marine Geosciences, University of Miami, 4600 Rickenbacker Cswy., Miami, FL 33149, USA*

[3]*Division of Polar Ocean Environment, Korea Polar Research Institute, 26 Songdomirae-ro, Yeonsu-gu, Incheon, 406-840, Republic of Korea*

Abstract. Interferometric synthetic aperture radar (InSAR) techniques can monitor water-level changes in wetlands with suitable coherence. RADARSAT-2 has many beam modes with varying system parameters to satisfy a wide range of applications. During data acquisition the SAR signals are digitized using eight-bit analog-to-digital converters followed by block adaptive quantization (BAQ) coding. Most RADARSAT-2 beam modes use three-bit BAQ but some modes use two-bit BAQ to accommodate larger data sets, including the wide multilook fine and wide ultrafine modes. These modes are attractive for surface monitoring applications due to good resolution over a wide swath. The two-bit BAQ can have signal saturation due to the smaller dynamic range and an increased phase noise. The Everglades National Park (ENP) has been used for numerous InSAR investigations of water level monitoring. This study describes the results of an evaluation of RADARSAT-2 products from different modes for the monitoring of water-level changes and flooded vegetation in ENP. The objective was to evaluate products from a variety of beam modes for wetland monitoring applications and subsequent unwrapping of the interferograms for water level estimation. The results show that wide-swath high-resolution modes are suitable for InSAR applications due to adequate coherence and high backscatter intensity.

Résumé. Les techniques InSAR peuvent suivre l'évolution du niveau de l'eau dans les zones humides avec une cohérence convenable. RADARSAT-2 a de nombreux modes de faisceaux avec différents paramètres du système pour répondre à une vaste gamme d'applications. Lors de l'acquisition des données, les signaux SAR sont numérisés à l'aide de convertisseurs analogiques/numériques de 8 bits suivis par un codage de la quantification adaptive de blocs (BAQ). La plupart des modes de faisceaux de RADARSAT-2 utilisent une BAQ de 3 bits, alors que certains modes utilisent une BAQ de 2 bits pour l'acquisition de plus grands ensembles de données, y compris les modes de faisceaux larges multivisées à résolution fine et de faisceaux larges à résolution ultra-fine. Ces modes sont attrayants pour les applications de surveillance de surface grâce à une bonne résolution sur une large fauchée. La BAQ à 2 bits peut montrer une saturation du signal en raison de sa gamme dynamique plus petite et d'un bruit de phase augmenté. Le Parc national des Everglades (ENP) a été utilisé pour de nombreuses études InSAR de la surveillance du niveau de l'eau. Cette étude décrit les résultats d'une évaluation des produits de RADARSAT-2 à partir de différents modes pour le suivi des changements du niveau de l'eau et de la végétation inondée dans l'ENP. L'objectif était d'évaluer les résultats à partir d'une variété de modes de faisceaux pour les applications de surveillance de zones humides et le déroulement ultérieur des interférogrammes pour l'estimation du niveau de l'eau. Les résultats montrent que les modes de faisceaux larges à haute résolution sont adaptés aux applications InSAR en raison de la cohérence adéquate et de la forte intensité de rétrodiffusion.

INTRODUCTION AND BACKGROUND

Interferometric synthetic aperture radar (InSAR) is an established technique that allows the mapping of terrain heights and surface deformation using two SAR images acquired with nearly identical system configurations by producing a phase interference image called an interferogram (Zebker and Goldstein 1986; Gabriel et al. 1989; Massonnet and Feigl 1998; Burgmann et al. 2000). Over the last couple of decades, this technology has been applied to a large number of applications, including tectonic deformation due to earthquakes (Massonnet et al. 1993), volcanoes (Rosen et al. 1996), ground subsidence due to water or oil extraction and mining activities (Tomás et al. 2005; Herrera et al. 2007), ice flow and glacier motion (Goldstein et al. 1993), and terrain stability due to permafrost (Short et al. 2011). It has also been used for monitoring urban environments and the stability of the infrastructure (Tomás et al. 2012) and other landscape features such as landslides (Herrera et al. 2010). Clearly

Received 27 October 2014. Accepted 18 August 2015.
*Corresponding author e-mail: shong@kopri.re.kr

this technology is well established in the earth sciences and is widely used for monitoring applications.

Recent research has demonstrated the use of InSAR technology for monitoring water-level changes in wetlands (Alsdorf et al. 2001; Wdowinski et al. 2004, 2008; Lu et al. 2005; Kim et al. 2009; Hong et al. 2010). The wetland InSAR technique works where vegetation emerges above the water surface due to the "double bounce" effect, in which the radar pulse is reflected twice from the water surface and from the vegetation (Richards et al. 1987). This approach has also been used for monitoring the tide propagation through coastal wetlands (Wdowinski et al. 2013). The results show that many wetlands with flooded vegetation remain coherent at all polarizations over a wide range of incidence angles and wavelengths (X-, C-, and L-bands). The longer wavelengths are preferred for woody wetlands and the shorter wavelengths for herbaceous wetlands, but this approach appears very promising for producing geospatial water level monitoring capability at relatively high resolution (10–40 m) compared to point source monitoring with gauges and other instruments. With future constellations and a proliferation of SAR data, it is possible to develop a surface water-level monitoring capacity with centimeter accuracy and weekly products. This would be useful to a number of applications including hydrology, environmental monitoring studies, weather forecasting, agriculture, etc.

The Everglades National Park (ENP) includes saltwater coastal wetlands along the western and southern shores of the park and freshwater wetlands further inland. This site has been used for numerous InSAR investigations related to water-level monitoring (Wdowinski et al. 2004, 2008; Hong et al. 2010) with the wetlands usually exhibiting suitable coherence for wetland InSAR monitoring applications with temporal coherence often approaching 72 days or longer (Kim et al. 2013). Some studies indicate that the InSAR application over the wetland shows very good performance to generate absolute water-level time series (Hong, Wdowinski, Kim, and Won 2010; Hong and Wdowinski 2014). These extensive wetlands with long-term coherence are a good location for InSAR-related research. In addition to the RADARSAT-1 heritage beam modes (fine, standard, wide, ScanSAR narrow, ScanSAR wide, extended low, and extended high), RADARSAT-2 offers ultrafine, multilook fine, fine quad-pol, and standard quad-pol beam modes. Additional modes including wide ultrafine, wide multilook fine, extrafine, and wide fine were added after launch. During RADARSAT-2 data acquisitions the SAR signals are digitized using eight-bit analog-to-digital converters followed by block adaptive quantization (BAQ) coding. The BAQ coding reduces on-board data storage and downlink rates and is capable of using from one- to four-bit representation for each in-phase (I) and quadrature phase (Q) value for the complex SAR data sample. During ground processing, the encoded samples are then decoded back to eight-bit representation with some information loss (MacDonald Dettwiler and Associates 2013). Most of the RADARSAT-2 beam modes use three-bit BAQ, but the wider swaths of some modes use two-bit BAQ to accommodate larger data sets. In particular, the wide multilook fine and wide ultrafine modes use this two-bit BAQ for data downloads. These modes are attractive for surface monitoring applications due to the relatively high resolution over a wide swath. One consequence of the two-bit BAQ download data is a possibility of signal saturation due to the smaller dynamic range and an increase in phase noise, making the unwrapping process difficult (McLeod et al. 1998). McLeod et al. (1998) pointed out that although a reduction from eight bits to four bits per sample in the download data was the maximum data reduction ratio for precision InSAR applications, three bits or two bits per sample was only appropriate for less demanding wide-swath applications.

This article describes the results of a comparison of RADARSAT-2 products from various modes for the InSAR measurement of water-level changes in vegetated wetlands. The objectives were to evaluate the various products for suitability for wetland monitoring including the coherence level and the ability to unwrap the interferogram. The results are then used to make recommendations on RADARSAT-2 beam mode selection for distributed target InSAR applications using RADARSAT-2 and, in particular, for water-level monitoring. The following sections describe the data used for the analysis, the data processing methodology, and the results and discussion of the suitability of the various modes and the impact of the two-bit downloads on InSAR applications, particularly water-level monitoring.

METHODOLOGY

Site Description

Our study area consists of the ENP in southern Florida (Figure 1), which is a remnant of a large wetland area that covered most of south Florida until the beginning of the 20th century, when humans settled the area and disrupted the natural flow regime. The ENP includes saltwater coastal wetlands along the western and southern shores of the park and freshwater wetlands further inland. The hydrology of the coastal wetlands is dominated by daily tidal flow, which propagates inland along tidal channels, whereas the hydrology of the inland freshwater wetlands is dominated by a wide, shallow sheetflow, known as the Everglades "river of grass" (Douglas 1947).

The vegetation in the study area includes both freshwater swamps and saltwater mangroves, with a variety of vegetation types comprising a very rich ecosystem. The freshwater swamps consist mainly of sawgrass (herbaceous vegetation) and islands of hardwood hammock (tree islands). In between the freshwater swamps and the saltwater mangroves, there is a transition zone with mixed vegetation, often termed prairies. The saltwater mangrove forests contain trees of variable height. Short mangroves are found in many locations around the park, whereas tall mangrove trees ($>$15 m high) are located mainly in the southwestern corner of the park (Simard et al. 2006) in areas dissected by numerous tidal channels.

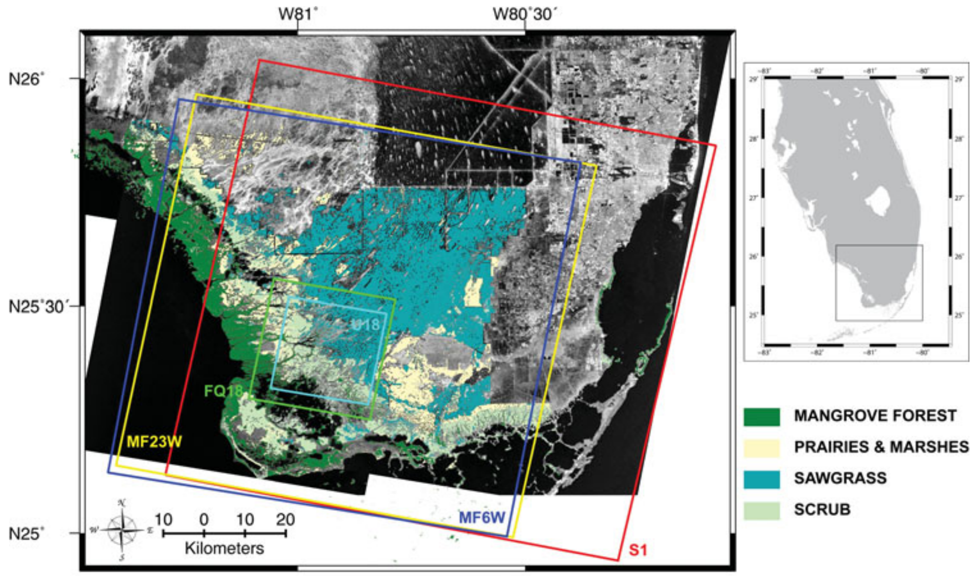

FIG. 1. SAR amplitude mosaic of the southern Florida Everglades showing the frame location of the five acquisition modes used in this study.

RADARSAT-2 Data

A series of RADARSAT-2 acquisitions of different beam modes was made of the ENP (Table 1). The time window was kept as small as possible to avoid temporal decorrelation and subsequent loss of coherence. All passes were descending right looking. The collected RADARSAT-2 interferometric pairs have small geometric, temporal, and Doppler centroid baselines from well-controlled operations enough to maintain the coherence of interferometric pairs. Table 2 provides a list of the RADARSAT-2 data acquired for this project.

Data Processing Methodology

The RADARSAT-2 data were processed using the Repeat Orbit Interferometry PACkage (ROI_PAC; Buckley et al. 2000) and Gamma Remote Sensing software package. For each acquisition mode we calculated interferograms with a 24-day time span, because wetland interferograms are most sensitive to the temporal baseline (S.-W. Kim et al. 2013). Wetland interferograms with longer spans (48 days and longer) are strongly affected by reduced coherence. For some acquisition modes (S1, FQ18, MF3F, and U18) we acquired and analyzed only a single pair with a 24-day temporal baseline. For the two other modes (MF6W and MF23W) we acquired more data and analyzed three 24-day interferograms for each acquisition mode. Unlike most InSAR studies, we present and analyze wrapped and unfiltered interferograms, because both operations tend to smear small signals in order to increase the signal-to-noise ratio due to spatial resolution.

Each interferometric pair acquired with various beam modes was coregistered using amplitude correlation coefficients. Multilooking of 4 was used to reduce the amount of noise in the interferograms. Differential interferograms were generated with topographic phase removal using SRTM-1 DEM, interferometric filtering (Goldstein and Werner 1998), and phase unwrapping. The coherence was estimated using a 5 × 5 window.

To evaluate the phase noise from different bit products of RADARSAT-2, we applied an interferometric technique as described in the Data Processing section. The calculated interferograms enable us to assess the quality of interferograms with visual interpretation in each beam mode acquisition. The quality of the interferogram is affected by decorrelation factors such as geometric, temporal, Doppler centroid baseline, coregistration errors during interferometric processing, signal-to-noise, etc. The collected RADARSAT-2 interferometric pair has small geometric, temporal, and Doppler centroid baselines from well-controlled operation enough to maintain the coherence of interferometric pairs.

Calculation of the coherence values is the most robust method to evaluate the quality of interferograms. Coherence analyses were conducted for all of interferograms with 5 × 5 pixels of estimation windows and the average coherence was calculated in the overall area. Because the coherence over wetland area is significantly degraded by the time span between two acquisitions (Hong, Wdowinski, and Kim 2010), we need to evaluate the coherence considering the effect of temporal baseline. It is reported that the coherence in the wetland has less dependence on the geometric perpendicular baselines compared to the temporal baseline decorrelation (Hong and Wdowinski 2012).

RESULTS

The geometric perpendicular baselines were small (<300 m) and the Doppler centroid baselines were stable for all inter-

TABLE 1
RADARSAT-2 C-band SAR beam mode parameters

Beam mode	Polarization	Pixel spacing	Scene size (km)	Incidence angle (°)	BAQ level (bits)
S1	HH/HV	Range: 7.99 m Azimuth: 5.12 m	100 × 100	24.72	3
FQ18	HH/HV/VH/VV	Range: 4.73 m Azimuth: 4.96 m	25 × 25	38.58	3
MF3F	HH	Range: 2.66 m Azimuth: 3.02 m	50 × 50	43.43	3
MF6W	HH	Range: 2.66 m Azimuth: 2.89 m	90 × 50	48.49	2
MF23W	HH	Range: 2.66 m Azimuth: 2.38 m	90 × 50	32.39	2
U18	HH	Range: 1.33 m Azimuth: 2.07 m	20 × 20	43.83	3
SLA11	HH	Range: 1.33 m Azimuth: 0.39 m	18 × 8	38.51	3

ferometric pairs. All of the interferograms with short temporal baselines (24 days) have sufficient coherence to observe the fringe pattern, which represents water-level changes occurring during the time span between two SAR acquisitions (Figures 2 and 3). Each fringe cycle reflects 2.7 cm of water-level change in line of sight between the satellite and the surface, which translates to roughly 4 cm of vertical change; the accurate value is inversely proportional to the acquisitions' incidence level (Table 1). Further details on the wetland InSAR application and related uncertainties (3–4 cm) can be found in previous studies (Wdowinski et al. 2004, 2008; Hong et al. 2010).

TABLE 2
RADARSAT-2 C-band SAR image acquisitions

Date	Time	Beam mode
20-Jul-12	11:10:54 AM	MF6W
23-Jul-12	11:23:21 AM	MF23W
30-Jul-12	11:19:18 AM	FQ18
06-Aug-12	11:15:10 AM	U18
09-Aug-12	11:27:28 AM	S1
13-Aug-12	11:10:54 AM	MF6W
16-Aug-12	11:23:21 AM	MF23W
23-Aug-12	11:19:18 AM	FQ18
30-Aug-12	11:15:10 AM	U18
02-Sep-12	11:27:28 AM	S1
06-Sep-12	11:10:54 AM	MF6W
09-Sep-12	11:23:21 AM	MF23W
30-Sep-12	11:10:54 AM	MF6W
03-Oct-12	11:23:21 AM	MF23W
10-Oct-12	11:19:19 AM	SLA11
17-Oct-12	11:15:07 AM	MF3F
24-Oct-12	11:10:54 AM	MF6W
27-Oct-12	11:23:21 AM	MF23W
03-Nov-12	11:19:19 AM	SLA11
10-Nov-12	11:15:07 AM	MF3F
17-Nov-12	11:10:54 AM	MF6W
20-Nov-12	11:23:21 AM	MF23W

In this study, we evaluate the quality and suitability of each acquisition mode for the wetland InSAR application, by visual comparison between interferograms and coherence maps, as well as quantitative coherence analysis of the derived coherence maps. Three of the acquisition modes (S1, MF6W, and MF23W) acquired data over a very wide area that covers most of the ENP (Figure 1). All three interferograms show high coherence in the freshwater wetlands located in the northern and the central part of the southern part of the interferograms. Each interferogram presents different fringe pattern, which reflect water-level changes in the freshwater wetlands, as well as some contribution from atmospheric noise. Low coherence levels are found in two areas, one located along the western section of the Everglades National Park and the other in a limited area east of the park, along the eastern side of the interferograms. The low coherence along the western coast occurs mainly due to decorrelation by tall mangrove vegetation, whereas the low coherence in the eastern side occurs in an agricultural area, due to rapid crop grow and land cultivation. Overall, the S1 interferogram shows the lowest coherence, whereas the MF6W and MF23W show similar coherence levels. In order to better assess coherence level, we zoom in to the vegetation transition area marked by the white frames in Figure 2.

The transition between freshwater and saltwater (mainly mangrove forests) in the western Everglades occurs over a wide area and follows irregular pattern mostly controlled by the loca-

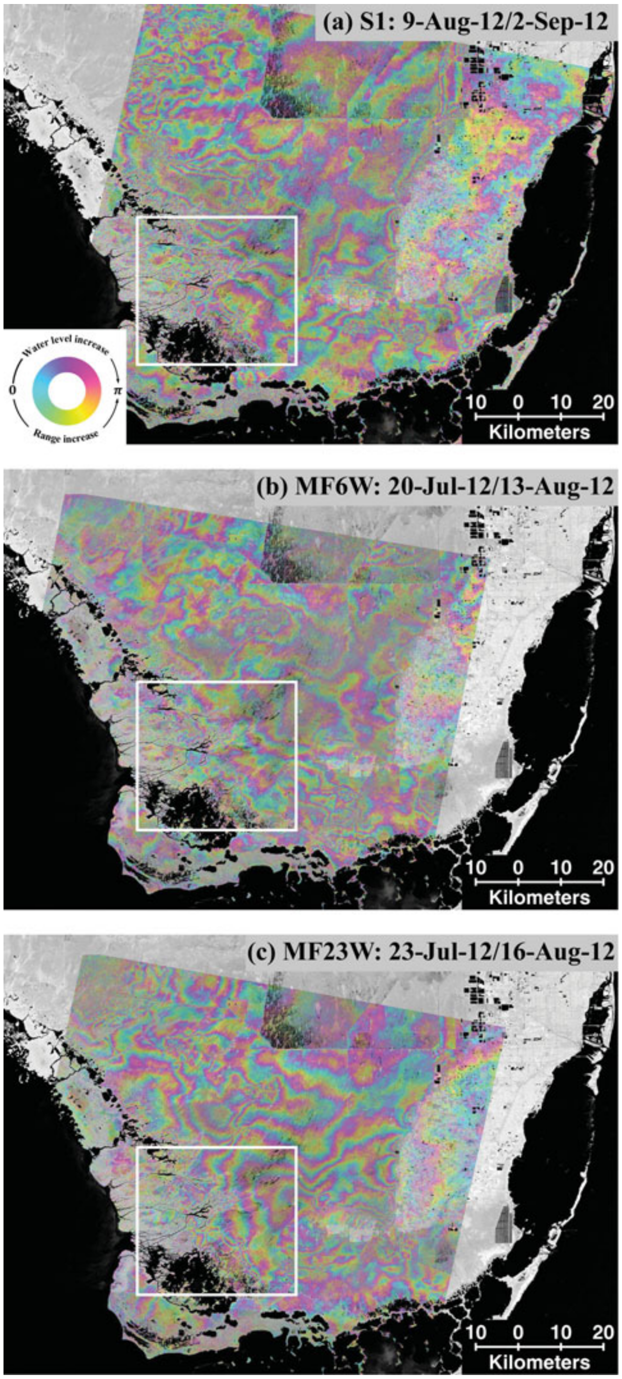

FIG. 2. Three representative interferograms covering most of Everglades National Park. The interferograms are wrapped and unfiltered to demonstrate the actual phase resolution detected by each acquisition mode. All interferograms show high coherence levels and variable fringe patterns in the freshwater wetlands located in the upper right side of the images. They also show low coherence over the mangrove forest area, on the left side of the interferograms. The white frames mark the location of the zoomed-in area presented in Figure 3.

tion of the tidal channels. Because coherence is mostly affected by the vegetation type, the irregular shape of the vegetation transition provides a good measure to evaluate the quality of the interferograms to resolve short wavelength features (<300 m); for example, water-level changes along tidal channels. Here we evaluate the three interferograms presented in Figure 2, as well as high-resolution interferograms acquired with modes FQ18 and U18. The interferograms presented in the zoomed-in area (Figure 3) show an overall similar pattern to that of the larger scale interferograms. The interferograms show high coherence over the freshwater wetlands in the northeastern section of the zoomed-in area and low coherence over tall mangrove forests in the southwestern sections. However, the coherence and short wavelength detection capability in the transition zone vary from one interferogram to the other. The S1 interferogram shows the worst coherence and detection capability, the MF6W and FQ18 interferograms show higher coherence but limited detection capability, and the U18 interferogram shows low coherence but high detection capability. The detection capability reflects the acquisition's spatial resolution. The highest detection resolution obtained with the U18 acquisition mode was obtained with a pixel resolution of 1–2 m. Intermediate detection level was obtained with the MF6W, MF23W, and FQ18 modes that were acquired with a pixel resolution of 2–5 m. The worst detection capability was obtained by the S1 mode with a pixel resolution of 5–8 m.

A direct measure of the interferometric coherence can be obtained from coherence maps. We calculated such maps for both the larger scale interferograms and of the zoomed-in area (Figure 4). The larger scale interferograms show a significantly higher coherence of the MF6W over the S1 acquisition mode. The MF23W shows a similar or even slightly better coherence than the MF6W mode. In the zoomed-in area, the highest coherence levels are obtained by the U18 and MF6W modes, intermediate by FQ18, and worst by S1 mode.

We used a visual evaluation to compare the coherence between the different acquisition modes. In order to obtain a quantitative comparison between the modes, we calculated the coherence level in the zoomed-in area for each acquisition mode according to the vegetation type, as well as for the entire zoomed-in area. The calculations are based on mean coherence values obtained for polygons dividing the area according to the main vegetation types (Figure 5). The results of the quantitative coherence analysis show that coherence levels of all vegetation and sensor types vary in the range of 0.3–0.4. This range reflects an intermediate coherence level that is usually sufficient to maintain phase observations. Typically, phase observations cannot be maintained when coherence level is below 0.2. Thus, our results suggest that all acquisition modes provide sufficient coherence for detecting water-level change.

Coherence levels vary among the various acquisition modes depending on the vegetation type. The MF23W has highest coherence levels for all vegetation types, the U18 and FQ18 modes show different coherence level in different veg-

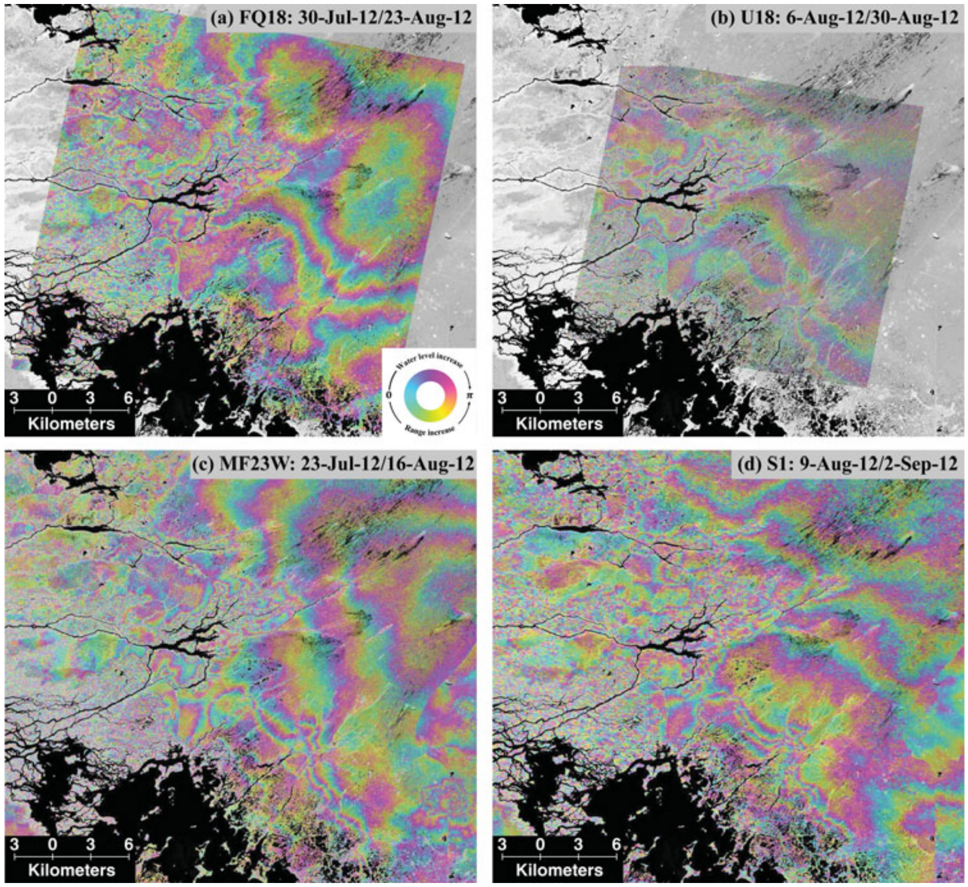

FIG. 3. Zoomed-in interferograms of the Tarpon Bay area, which is a transition zone between freshwater wetlands to the northeast and mangrove forests in the southwest. The Tarpon Bay and other tidal channels in the area are homes for the easternmost mangrove communities in the western Everglades. The interferograms show high coherence with low fringe gradients in the northeast area, which reflect water-level changes in the steady flowing freshwater wetlands. They also show low coherence over the mangrove forests in the southwest sections. Some of the interferograms also show high gradient fringes around the Tarpon Bay, reflecting water-level changes induced by tidal flow.

etation types, and the MF6W and S1 modes show, overall, the lowest coherence levels (Figure 6). The results indicate that the BAQ level is not a main contributor to the coherence level. The highest and intermediate coherence were detected in BAQ level 2 interferograms (MF23W, MF6W) at similar coherence levels to BAQ level 3 interferograms (U18, FQ18, S1). Furthermore, the comparative coherence analysis suggests some degree of coherence sensitivity to spatial resolution, in which higher coherence levels occur in higher resolution interferograms.

DISCUSSION

The ENP wetland interferograms demonstrate suitable coherence values for InSAR water-level monitoring, which has enabled our comparison of beam modes for this application using RADARSAT-2 data. The results show similar coherence levels in the BAQ level 2 and 3 interferograms, which indicate that the smaller dynamic range of the BAQ 2 backscattering signal is sufficient for monitoring water-level changes over wetlands environments. The smaller dynamical range is sufficient, because the transitions between the different wetland vegetation types tend to be continuous and smooth. Consequently, saturation of the signal and phase noise issues is not a problem for this type of application because of adequate signal-to-noise for wetland InSAR.

In this study we solely evaluated the effect of the acquisition mode, in particular the BAQ level, on the interferometric coherence, as a quality measure of wetland InSAR application. Consequently, we ignored other possible decorrelation effects as geometrical baseline, temporal disturbances, and acquisition geometry (incidence angle). However, our previous thorough coherence analysis over wetlands indicated that interferometric coherence is dominated by temporal baseline, whereas all other decorrelating effects play minor roles (Kim et al. 2013). Because we restricted our coherence analysis to 24-day interferograms, we eliminated the main decorrelation source from the analysis.

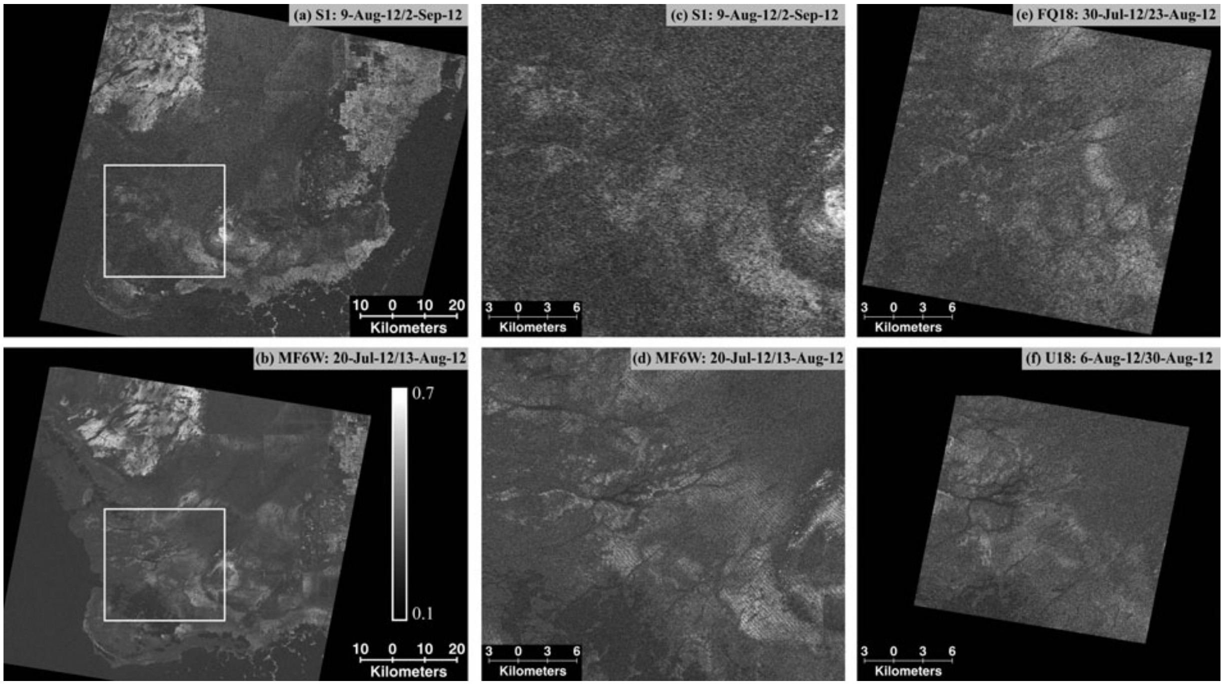

FIG. 4. Coherence maps based on the interferograms presented in Figures 2 and 3. The maps in (a) and (b) show the coherence in the entire frames of the S1 and MF6W, respectively. The white frames mark the location of the zoomed-in area around Tarpon Bay presented in (c) and (d). Coherence map of the higher resolution FQ18 and U18 acquisition modes are shown in (e) and (f), respectively.

The contribution of other decorrelation effects are minor and do not change the main result of our analysis, indicating that BAQ level 2 interferograms have coherence similar to BAQ level 3 interferograms.

The results of our study are good news because the wide swath (approximately 100 km) with moderate resolution (2–5 m) is an attractive option for surface water and wetland monitoring applications. Thus, for RADARSAT-2 the wide multilook fine

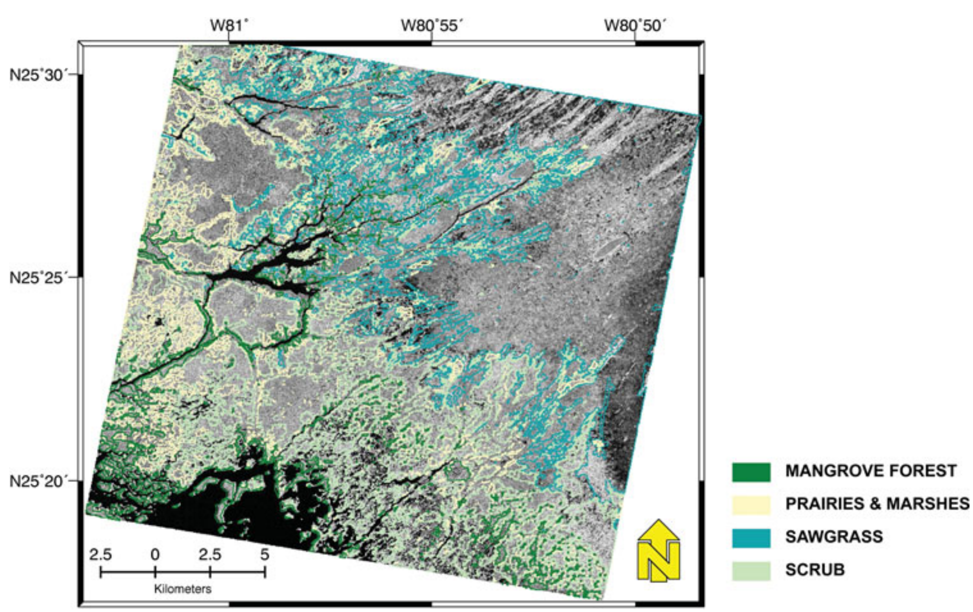

FIG. 5. RADARSAT-2 amplitude image with polygons of vegetation class that is used for coherence calculation.

modes with two-bit BAQ downloads may provide the best trade-off in area coverage versus data quality for this application. In the near future with constellations such as the RADARSAT Constellation Mission providing more frequent observations, it is quite conceivable to develop a surface water monitoring system with weekly observations providing surface water extent, flooded vegetation, and water-level change information. The higher repeat observations will provide timely output from the end-user perspective while maintaining good coherence due to the short temporal baseline.

SUMMARY

This article describes the results of a comparison of RADARSAT-2 products from various beam modes for the InSAR measurement of water-level changes in vegetated wetlands in ENP. The objective was to evaluate the suitability of the different products including the phase noise and saturation issues of the two-bit products when compared to the three-bit products. The results show that the adequate signal-to-noise in vegetated wetlands accommodates the use of two-bit BAQ downloads for InSAR applications such as water-level monitoring. This is good news because the wide swath (approximately 100 km) with moderate resolution (2–5 m) is an attractive option for surface water and wetland monitoring applications. Thus, for RADARSAT-2 the wide multilook fine modes with two-bit BAQ downloads may provide the best trade-off in area coverage versus data quality for this application. In the near future with constellations such as the RADARSAT Constellation Mission providing more frequent observations, it is quite conceivable to develop a surface water monitoring system with weekly observations providing surface water extent, flooded vegetation, and water-level change information. The higher repeat observations will provide timely output from the end-user perspective while maintaining good coherence due to the shorter temporal baseline.

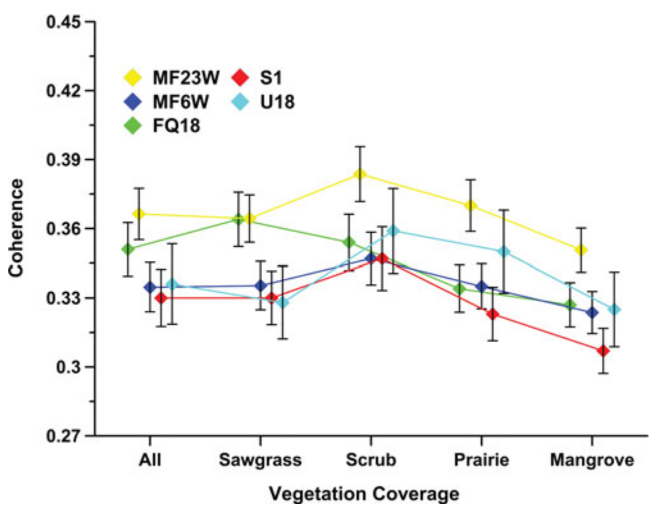

FIG. 6. Coherence analysis of the various acquisition modes presented according to vegetation type. The analysis is based on several interferograms with the MF23W and MF6W acquisition modes.

ACKNOWLEDGMENTS

Thanks to Sergey Samsonov and Naomi Short for critical reviews of the article.

FUNDING

This research project was supported by the RSS program at ESS/CCMEO/CCRS and the CSA through the RCM-CCD funding. S.W. is grateful for support from the NASA Cooperative Agreement No. NNX10AQ13A (WaterSCAPES: Science of Coupled Aquatic Processes in Ecosystems from Space) and the Florida Coastal Everglades Long-Term Ecological Research program under National Science Foundation Grant No. DEB-1237517. S.H. is grateful for support from the KOPRI project (PE15040).

REFERENCES

Alsdorf, D., Smith, L., and Melack, J. 2001. "Amazon floodplain water level changes measured with interferometry SIR-C radar." *IEEE Transactions on Geoscience and Remote Sensing*, Vol. 39: pp. 423–431.

Buckley, S.M., Rossen, P.A., and Persaud, P. 2000. *ROI_PAC Documentation—Repeat Orbit Interferometry Package*. Pasadena, CA: JET Propulsion Lab.

Burgmann, R., Rosen, P.A., Fielding, E.J. 2000. "Synthetic aperture radar interferometry to measure Earth's surface topography and its deformation." *Annual Review of Earth and Planetary Sciences*, Vol. 28: pp. 169–209.

Douglas, M.S. 1947. *The Everglades: River of Grass*. St. Simonds Island, GA: Mockingbird Books.

Gabriel, A.K., Goldstein, R.M., and Zebker, H.A. 1989. "Mapping small elevation changes over large areas—Differential radar interferometry." *Journal of Geophysical Research*, Vol. 94: pp. 9183–9191.

Goldstein, R.M., Engelhardt, H., Kamb, B., and Frolich, R.M. 1993. "Satellite radar interferometry for monitoring ice sheet motion: Application to an Antarctic ice stream." *Science*, Vol. 262 (No. 5139): pp. 1525–1530.

Goldstein, R.M., and Werner, C.L. 1998. "Radar interferogram filtering for geophysical applications." *Geophysical Research Letters*, Vol. 25 (No. 21): pp. 4035–4038.

Herrera, G., Tomás, R., Lopez-Sanchez, J.M., Delgado, J., Mallorqui, J.J., Duque, S., and Mulas, J. 2007. "Advanced DInSAR analysis on mining areas: La Union case study (Murcia, SE Spain)." *Engineering Geology*, Vol. 90: pp. 148–159.

Herrera, G., Tomás, R., Vicente, F., Lopez-Sanchez, J.M., Mallorquí, J.J., and Mulas, J. 2010. "Mapping ground movements in open pit mining areas using differential SAR interferometry." *International Journal of Rock Mechanics and Mining Sciences*, Vol. 47: pp. 1114–1125.

Hong, S.-H., and Wdowinski, S. 2012. "Evaluation of the quad-polarimetric RADARSAT-2 observations for the wetland InSAR application." *Canadian Journal of Remote Sensing*, Vol. 37: pp. 484–492.

Hong, S.-H., and Wdowinski, S. 2014. "Multitemporal multitrack monitoring of wetland water levels in the Florida Everglades using ALOS PALSAR data with interferometric processing." *IEEE Geoscience and Remote Sensing Letters*, Vol. 11: pp. 1355–1359.

Hong, S.-H., Wdowinski, S., and Kim, S.-W. 2010. "Evaluation of TerraSAR-X observations for wetland InSAR application." *IEEE Transactions on Geoscience and Remote Sensing*, Vol. 48 (No. 2): pp. 864–873.

Hong, S.H., Wdowinski, S., Kim, S.W., and Won, J.S. 2010. "Multi-temporal monitoring of wetland water levels in the Florida Everglades using interferometric synthetic aperture radar (InSAR)." *Remote Sensing of Environment*, Vol. 114: pp. 2436–2447.

Kim, J.W., Lu, H., Lee, C.K. Shum, C.M., Swarzenski, T.W., Doyle, Z. and Baek, S.-H. 2009. "Integrated analysis of PALSAR/RADARSAT-1 InSAR and ENVISAT altimeter data for mapping of absolute water level changes in Louisiana wetlands." *Remote Sensing of Environment*, Vol. 113: pp. 2356–2365.

Kim, S.-W., Wdowinski, A., Amelung, T.H., Dixon, S. and Won, J.-S. 2013. "Interferometric Coherence Analysis of the Everglades Wetlands, South Florida." *IEEE Transactions on Geoscience and Remote Sensing*, Vol. 51: pp. 1–15.

Lu, Z., Crane, M., Kwoun, O., Wells, C., Swarzenski, C., and Rykhus, R. 2005. "C-band radar observes water level change in swamp forests." *EOS, Transactions American Geophysical Union*, Vol. 86: pp. 141–144.

MacDonald Dettwiler and Associates. 2013. *RADRSAT-2 Product Description, RN-SP-52-1238*. Richmond, BC, Canada: MacDonald Dettwiler and Associates Ltd.

Massonnet, D., and Feigl, K.L. 1998. "Radar interferometry and its application to changes in the Earth's surface." *Reviews of Geophysics*, Vol. 36: pp. 441–500.

Massonnet, D., Rossi, M., Carmona, C., Adragna, F., Peltzer, G., Feigl, K., and Rabaute, T. 1993. "The displacement field of the Landers earthquake mapped by radar interferometry." *Nature*, Vol. 364: pp. 138–142.

McLeod, I.H., Cumming, I.G., and Seymour, M.S. 1998. "ENVISAT ASAR data reduction: Impact on SAR interferometry." *IEEE Transactions on Geoscience and Remote Sensing*, Vol. 36: pp. 589–602.

Richards, J.A., Woodgate, P.W., and Skidmore, A.K. 1987. "An explanation of enhanced radar backscattering from flooded forests." *International Journal of Remote Sensing*, Vol. 8: pp. 1093–1100.

Rosen, P.A., Hensley, S., Zebker, H.A., Webb, F.H., and Fielding, E.J. 1996. "Surface deformation and coherence measurements of Kilauea Volcano, Hawaii, from SIR C radar interferometry." *Journal of Geophysical Research*, Vol. 101 (No. E10): pp. 109–123, 126.

Short, N., Brisco, B., Couture, N., Pollard, W., Murnaghan, K., and Budkewitsch, P. 2011. "A comparison of X-, C- and L-band SAR interferometry for monitoring permafrost environments, case study from Herschel Island, Canada." *Remote Sensing of Environment*, Vol. 115: pp. 3491–3506.

Simard, M., Zhang, K.Q., Rivera-Monroy, V.H., Ross, M.S., Ruiz, P.L., Castaneda-Moya, E., Twilley, R.R., and Rodriguez, E. 2006. "Mapping height and biomass of mangrove forests in Everglades National Park with SRTM elevation data." *Photogrammetric Engineering and Remote Sensing*, Vol. 72 (No. 3): pp. 299–311.

Tomás, R., García-Barba, J., Cano, M., Sanabria, M.P., Ivorra, S., Duro, J., and Herrera, G. 2012. "Subsidence damage assessment of a gothic church using differential interferometry and field data." *Structural Health Monitoring*, Vol. 11: pp. 751–762.

Tomás, R., Márquez, Y., Lopez-Sanchez, J.M., Delgado, J., Blanco, P., Mallorquí, J.J., Martínez, M., Herrera, G., and Mulas, J. 2005. "Mapping ground subsidence induced by aquifer overexploitation using advanced differential SAR interferometry: Vega Media of the Segura River (SE Spain) case study." *Remote Sensing of Environment*, Vol. 98: pp. 269–283.

Wdowinski, S., Amelung, F., Miralles-Wilhelm, F., Dixon, T.H., and Carande, R. 2004. "Space-based measurements of sheet-flow characteristics in the Everglades wetland, Florida." *Geophysical Research Letters*, Vol. 31 (No. 15): p. L15503.

Wdowinski, S., Hong, S.-H., Mulcan, A., and Brisco, B. 2013. "Remote-sensing monitoring of tide propagation through coastal wetlands." *Oceanography*, Vol. 26 (No. 3): pp. 64–69. http://dx.doi.org/10.5670/oceanog.2013.46.

Wdowinski, S., Kim, S.W., Amelung, F., Dixon, T.H., Miralles-Wilhelm, F., and Sonenshein, R. 2008. "Space-based detection of wetlands' surface water level changes from L-band SAR interferometry." *Remote Sensing of Environment*, Vol. 112: pp. 681–696.

Zebker, H., and Goldstein, R. 1986. "Topographic mapping from SAR observation." *Journal of Geophysical Research*, Vol. 911: pp. 4993–4999.